P.O.L.

PHYSICAL AND DYNAMICAL PROPERTIES OF LUNDY SAND

BY
J.J. WILLIAMS

REPORT NO. 3
1988

NATURAL ENVIRONMENT RESEARCH COUNCIL
PROUDMAN OCEANOGRAPHIC LABORATORY

PROUDMAN OCEANOGRAPHIC LABORATORY

Bidston Observatory
Birkenhead, Merseyside, L43 7RA, U.K.
Tel: 051 653 8633
Telex: 628591OCEANSB
Fax: 051 653 6269

Director: Dr. B.S. McCartney

Natural Environment Research Council

PROUDMAN OCEANOGRAPHIC LABORATORY

REPORT No. 3

Physical and dynamic properties of Lundy sand

J J Williams

1988

DOCUMENT DATA SHEET

AUTHOR
J J WILLIAMS

PUBLICATION DATE 1988

TITLE
Physical and dynamic properties of Lundy sand

REFERENCE
Proudman Oceanographic Laboratory Report, No. 3, 30pp

ABSTRACT

This report presents data on the physical (grain size, shape, density and mineralogy) and dynamic (settling velocity and entrainment threshold) characteristics of sediment collected during the deployment of STABLE on a sand bank off Lundy Island (51°11.8'N, 04°42.5'W) on 30.09.87. Comparison is made between these results and published data.

This work has been carried out in connection with a contract to the Ministry of Agriculture, Fisheries and Food. The results may be used in the formulation of Government policy, but at this stage they do not necessarily represent Government policy.

ISSUING ORGANISATION
Proudman Oceanographic Laboratory
Bidston Observatory
Birkenhead, Merseyside L43 7RA
UK

Director: Dr B S McCartney

TELEPHONE 051 653 8633

TELEX 628591 OCEAN BG

TELEFAX 051 653 6269

KEYWORDS
LUNDY ISLAND
SAND
GRAIN SIZE
SETTLING VELOCITY
SEDIMENT ENTRAINMENT
THRESHOLD

CONTRACT

PROJECT PK94

PRICE £11.00

Copies of this report are available from:
The Library, Proudman Oceanographic Laboratory.

CONTENTS **PAGE**

1.0 INTRODUCTION

It is well known that when waves are superimposed on a steady tidal current, greatly enhanced sediment transport rates result owing to both stirring effects induced by vortex shedding and the high instantaneous bed shear stresses generated in the very thin wave boundary layer, DYER (1986). Although wave motion by itself cannot produce net sediment transport, (except a minor flux termed Stokes' drift), it is extremely effective in placing sediment into suspension where relatively weak currents can produce considerable net transport. Despite the significance of combined wave/current boundary layer processes in sediment transport, laboratory and field data representing the wide range of naturally encountered conditions are sparse and inconclusive and generally the calculation of the net sediment flux is based on inappropriate current-only transport equations with a resulting underestimation of net transport. It is therefore desirable to extend work on sediment transport in combined wave/current situations so that more physically realistic prognostic models can be developed. A research program to achieve these objectives is funded by the Ministry of Agriculture, Fisheries and Food and is undertaken collaboratively by Hydraulics Research Ltd., The Proudman Oceanographic Laboratory and University College North Wales.

Initial work was undertaken during September 1986 using the STABLE rig (HUMPHERY, 1987) on an area of non-erosive gravel South West of the Isle of Wight. Useful data regarding the wave/current/sediment interactions on an immobile sea bed were obtained. In order to obtain data regarding wave/current/sediment interactions on an erosive bed STABLE was redeployed on an active sandbank off the North West tip of Lundy on 30.09.87 (Figure 1). An initial sidescan survey of this area (WILKINSON & WAINWRIGHT, 1983) showed the bank shallowing from South East to North West with no distinguishable bedforms present. Subsequent surveys by ship echo sounder and diving reconnaissance, however, have indicated the presence of large-scale low amplitude bedforms and ripples covering significant portions of the bank. It therefore appears that the area is subject to modification (probably during storms) and is thus a sufficiently dynamic environment for the present study. The instrumentation used in this deployment is summarised in Table 1. Instrument interrogation and data recording is controlled by a programmed dual function Sea Data Logger and integral d.c. power supply (HUMPHERY, 1987).

The purpose of this short investigation has been to quantify the basic physical and dynamic properties associated with sediments at the Lundy deployment site. Such data will be required in subsequent analysis of the acoustic backscatter signals and the hydrodynamic data.

1.1 Sample collection

During deployment of STABLE, divers collected two surface sand samples from areas close to the rig. Shipek grab samples of the bed material were also taken at four sites close to STABLE. In addition, approximately 30 grab samples were collected en masse as the vessel drifted away from STABLE. For convenience these samples are referred to as S_1 and S_2 (surface samples), G_1, G_2, G_3 and G_4 (grab samples) and BLK (bulk sample) respectively in the following analysis and discussion.

2.0 PHYSICAL PROPERTIES

By examination of the sediment mineralogy using a polarizing microscope it was found that the majority of mineral grains were composed of quartz with small amounts of feldspars, zircon, tourmaline and shell fragments (see 2.2). The mean density of samples was found to be $2.642 gcm^{-3}$.

2.1 Grain size analysis by dry sieving

Grain size analysis by dry sieving was performed on all samples at Liverpool University. After thorough washing in distilled water to remove salt, samples were oven dried at 110°C for 24 hours. Sub-samples weighing approximately 100 grams were then obtained using a riffel box and sieved for $\frac{1}{2}$ hour using a mechanical sieve shaker and an appropriate sieve nest. Sieved fractions were weighed to an accuracy ±0.01 gram and the results plotted in the form grain size ($\phi = -Log_2 d, mm$) versus cumulative percent (probability scale). The characteristic asymptotic grain size distribution curves are shown in Figure 2.

The mean (d), standard deviation (σ_d), skewness (SK_d) and kurtosis (Ku_d) associated with each cumulative/phi plot were calculated by substituting appropriate values from the graphs into the following formulae (FOLK, 1974).

Graphic mean, $d = (\phi 16 + \phi 50 + \phi 84)/3$ (1)

Inclusive graphic standard deviation, σ_d =

$$\left[\frac{\phi 84-\phi 16}{4} \right] + \left[\frac{\phi 95-\phi 5}{6.6} \right] \quad (2)$$

Inclusive graphic skewness, SK_d =

$$\left[\frac{\phi 16+\phi 84-2\phi 50}{2(\phi 84-\phi 16)} \right] + \left[\frac{\phi 5+\phi 95-2\phi 50}{2(\phi 95-\phi 5)} \right] \quad (3)$$

Inclusive graphic kurtosis, $Ku_d = \frac{\phi 95-\phi 5}{2.44(\phi 75-\phi 25)}$ (4)

A summary of these statistics is presented in Table 2 and indicates that sediment from the sea bed near the STABLE deployment site may be classified as a very well sorted fine sand (d = 2.00ϕ , 250μm) characterised by a near symmetrical size distribution and strongly leptokurtic kurtosis. Such statistical properties are typical of a very well sorted, unimodal sediment.

2.2 Total carbonates

Visual inspection of the various sieve fractions indicated the presence of shell fragments. Quantification was obtained by the following analysis. A 15% solution of hydrochloric acid was added to 60g of each sediment sample. Although visible effervescence stopped after approximately two hours the samples were continuously agitated for 12 hours to ensure that all carbonates were completely dissolved. Samples were then washed in distilled water and oven dried at 110°C for 24 hours. The percentage of carbonates by weight in each sample was then determined, (Table 3). The mean size distribution associated with a carbonate free sample was then found by dry sieving a sample prepared by combining all the HCl treated sediments (Figure 3). In addition the percentage of total carbonates present in each sieve fraction was also found using a representative sample (Figure 4).

2.3 Roundness and sphericity

As the roundness and sphericity of grains significantly influence their hydraulic behaviour, a visual assessment of these properties was undertaken using

the descriptive indices suggested by KRUMBEIN & SLOSS (1963). In general, the relatively coarse particles consisting of marine faunal materials (predominantly shell fragments), were characterised by high angularity (0.1 to 0.3) and low sphericity (0.3 to 0.5). The significantly smaller quartz grains, however, were found to be sub-rounded/rounded (0.6 to 0.9) and characterised by relatively high sphericity (0.8 to 0.9). A sketch of typical faunal fragments and quartz grains is shown in Figure 5. These observations indicate that the hydraulic behaviour associated with the majority of grains within a given sample is unlikely to deviate significantly from that of spheres, (see 3.1).

2.4 Material in suspension

Suspended sediment samples were taken at 5 fixed heights during a 35 minute period of maximum ebb tide flow. The sampling apparatus consisted of an array of drogue nets (100μm sieve cloth) attached to a stainless steel rod. Substantial lead ballast ensured the apparatus remained vertical on the sea bed. The mouths of the drogues were held open by semi-rigid plastic rings which swivelled on the rod thus allowing the drogues to align themselves with the current.

On recovery, collected material was simply washed out of the drogues and stored for subsequent analysis. Samples from all the drogues contained a large portion of organic material (largely marine algae). This was removed prior to analysis using hydrogen peroxide. Only the bottommost trap (27.5cm above bed) contained sufficient sediment for dry sieve analysis (2.1). The statistical properties of the grain size distribution were found to be: $d=1.980$; $\sigma_d=0.2060$; $SK_d=0.232$; and $Ku_d=0.961$ (Figure 6). Although only small amounts of material were in suspension during the relatively calm weather on 30.09.87, the results show that the grain size distribution closely resembles those in Figure 2. During storm conditions, therefore, it is highly probable that all grain sizes are present in the water column.

Figure 7 shows the height distribution of suspended material during drogue deployment and shows that only very small amounts of material were present at heights above 0.5m in the flow conditions on that day. It was not possible to calculate net suspended sediment transport rates using this data as nothing is known about drogue collection efficiency. The deployment did, however, prove the feasibility of this technique for measuring net suspended sediment flux and

further work to produce a practical design for use in marine conditions is currently being undertaken.

3.0 DYNAMIC PROPERTIES

3.1 Grain size distribution and settling velocity using a settling column

The grain size and settling velocity distribution for each of the seven samples was determined using the settling column facilities at UCNW Menai Bridge. Data collection and analysis was automated and the errors associated with non-uniform sample introduction and wall effects were largely eliminated by correction factors in the processing software.

The grain size distribution estimates for each sample are shown in Figure 8. These data were obtained from the settling velocity values by assuming the grains to be spherical (see 2.3) and grain density to be $2.65gcm^{-3}$. Also included are the distribution statistics (mean, sorting (standard deviation), skewness and kurtosis, from FOLK, 1974) and the classification of the sediment according to WENTWORTH (1922). Close agreement is found between these results and those obtained by dry sieve analysis (2.1).

The mean characteristic settling velocity distribution for surface and grab samples are shown in Figure 9. These graphs show that although mean settling velocity for the whole sample ranged between $1.8cms^{-1}$ and $9.2cms^{-1}$, the mean settling velocity range associated with 80% of the sample by weight was only $2.9cms^{-1}$ to $3.8cms^{-1}$ for the surface samples (Figure 9a) and $2.9cms^{-1}$ to $4.1cms^{-1}$ for the grab samples (Figure 9b). In both cases these results reflect the considerable hydraulic similarity of grains. These data are in good agreement with data from LANE (1938), ENGELUND & HANSEN (1967), MOTLOVY & SYLVESTER (1979) and BABA & KOMAR (1981).

3.2 Entrainment and suspension threshold

Experiments to determine the entrainment and suspension threshold for Lundy sand were carried out using the tilting flume at The Civil Engineering Department, University of Liverpool. Three bed configurations were examined: (a) Flat bed; (b) asymmetrical ripples; and (c) symmetrical ripples. Measurements of

the three orthogonal flow components (u',w',v') were taken close to the bed using a LASER doppler anemometer (LDA) sampling at 100Hz. The resulting data were used to compute mean Reynolds stresses at threshold and at different degrees of transport intensity. In addition, a miniature discoidal electromagnetic current meter (ECM) was used to measure mean flow velocity above the LDA at mid-water, (Figure 10a).

(a) Flat bed

After careful levelling of the sediment bed and removal of any entrapped air the current velocity was increased. At threshold, entrained particles were illuminated by the LASER beams and were clearly visible as small bright flashes of light. The onset of such flashes was considered to represent the threshold condition for the sediment bed and thus the subjectivity normally associated with visual assessment of threshold conditions was reduced to an acceptable level.

Shell fragments were the first particles to move on the bed and these tended to roll and slide downstream. At slightly higher velocities, infrequent sporadic motion of both shell fragments and sand grains was recorded. Such movement often ceased a short distance downstream (<5cm). Further increases in velocity resulted in greater amounts of entrainment until ripple formation began and grains entered into suspension.

In runs 1 to 4 (Table 4), LDA measurements were taken at 0.2cm above the bed. It was found, however, that during the 20 second recording period of run 4, up to 65% of the flow records were unusable owing to sediment flux blocking the LASER beams. To overcome this the bed was re-flattened and the LDA repositioned at 5mm above the bed for runs 5 and 6. It was then possible to obtain a suitable data set for flow conditions during intense bedload transport (Table 4).

N.B. Velocity profiles taken at near threshold flow conditions showed that the constant stress layer extended to at least 10mm above the bed and thus assumptions made regarding the relationship between Reynold stress and bed shear stress remain valid.

(b) Asymmetrical ripples

Ripple formation described above was allowed to proceed for ½ hour in a steady current and gave rise to a series of asymmetrical ripples (Figure 10b). Following reduction in the flow velocity to below threshold the LASER intersection point was relocated 5mm above the crest of a ripple in the centre of the flume. Measurement of u', w' and v' were then taken at 3 levels of entrainment intensity using the LDA, (Table 4). In this case, 95% of LDA measurements were valid even during the most intense transport stage (Run 9).

(c) Symmetrical ripples

During the deployment of STABLE the divers observed fairly symmetrical ripples on the backs of other larger low amplitude bedforms. Using the wave generator in the flume it was possible to produce a near symmetrical series of vortex ripples with wavelength (≃10cm) and amplitude (≃3cm) closely resembling those recorded in the field (Figure 10c). The wave generator was then switched off and the LDA was positioned 5mm above the crest of a ripple in the centre of the flume. The procedure described in 3.2(a) was then followed and flow component measurements taken at two levels of entrainment intensity (Table 4).

3.3 Threshold results

Results of threshold runs 1 to 11 are given in Table 5. Shields criterion and grain Reynolds number were calculated by assuming: grain density $\sigma=1.65 gcm^{-3}$; fluid density $\rho=1.0 gcm^{-3}$; $g=981.0 cms^{-2}$; median grain diameter $d_{50}=0.025cm$; and kinematic viscosity $\nu=1.16\times10^{-6} m^2 s^{-1}$. The ECM U_{*T} values were calculated from U_{50} values using the Von Karman-Prandtl Law by assuming Z_o for the flat bed to be $1/30 d_{50}$ ($=8.3\times10^{-4}cm$). The results are in good agreement with U_{*T} values derived from LDA measurements of Reynolds stress, $(-u'w')^{\frac{1}{2}}$.

Figure 11 shows Shields criterion versus grain Reynolds number and includes published and experimental threshold data. The curve over this range of grain Reynolds number is given by MILLER et al. (1977) and is based on data for sand given by KRAMER (1935), CASEY (1935) and USWES. The experimental data plot as a diagonal line across the face of Shields curve with minimum and maximum Θ_T/Re^* values associated with threshold and suspension conditions respectively.

Experimental data associated with a moderate degree of bed motion agree well with published data despite uncertainty regarding entrainment criteria. It may also be noted that for a similar degree of entrainment, U_{*_T} values associated with the rippled beds are lower than those for the flat bed. This is considered to be the result of higher incident instantaneous shear stresses brought about by enhanced flow turbulence over ripples and by the greater degree of particle exposure to flow on the ripple crests, (DAVIES & WILKINSON, 1978).

4.0 SUMMARY

The following physical and dynamic properties were determined for sediment collected in the vicinity of the STABLE deployment site, Lundy.

1. Approximately 86% of the sediment by weight is composed of quartz grains. Other constituents include: faunal fragments (predominantly shell); feldspar; zircon; and tourmaline.

2. Mean sediment density was found to be $2.642 gcm^{-3}$.

3. The sediment was classified as a very well sorted, unimodal fine sand with graphic mean grain size equal to 2.00 ø (250μm).

4. Total mean carbonate content (largely shell) was found to be 12.4% by weight.

5. The degree of roundness associated with shell fragments and mineral grains was found to be 0.2 and 0.8 respectively whilst the sphericity of shell fragment and mineral grains was 0.4 and 0.8 respectively.

6. Similar grain size distributions were found for both suspended and static bed sediment.

7. The mean settling velocity was determined to be $3.35 cms^{-1}$.

8. Sediment entrainment threshold for a flat bed, asymmetrical ripples and symmetrical ripples was found to be $1.30 cms^{-1}$, $1.28 cms^{-1}$ and $1.16 cms^{-1}$ respectively.

4.1 Acknowledgements

The author wishes to acknowledge the Ministry of Agriculture, Fisheries and Food for part funding of this work. Thanks are extended to Professor Brian O'Conner, Terry Hedges, Ian Hale and Alan Moorhouse at The Civil Engineering Department, Liverpool University for advice and help on sediment analysis and LDA. Thanks also to Dr Colin Jago and Piers Larcombe at UCNW Menai Bridge for valuable help with settling velocity analysis.

4.2 References

BABA, J. & KOMAR, P.D. 1981. Measurements and analysis of settling velocities of natural quartz sand grains.
Journal Sedimentary Petrology, 51, 631-640.

CASEY, H.J. 1935. Über Geschiebebeuregung.
Mitteilungen der Preussischen Versuchsanstalt fur Wasserbau und Schiffbau, Berlin.

DAVIES, A.G. & WILKINSON, R.H. 1977. The movement of non-cohesive sediment by surface water waves. Part 1. Literature survey.
Institute of Oceanographic Sciences, Report No.45, 73pp.

DYER, K.R. 1986. Coastal and estuarine sediment dynamics.
Chichester: John Wiley. 342pp.

ENGELUND, F. & HANSEN, E. 1967. A monograph of sediment transport in alluvial streams.
Copenhagen: Technisk Vorlag. 62pp.

FOLK, R.L. 1974. Petrology of sedimentary rocks.
Texas: Hemphill.

HOTTOVY, J.D. & SYLVESTER, N.D. 1979. Drag coefficients for irregularly shaped particles.
Industrial and Engineering Chemistry Process Design and Development, 18, 433-436.

HUMPHERY, J.D. 1987. STABLE - an instrument for studying current structure and sediment transport in the benthic boundary layer.
pp.57-62 in, Fifth International Conference on Electronics for Ocean Technology, Herriot-Watt University, Edinburgh, 1987. London: Institution of Electronic and Radio Engineers. 225pp. (IERE Publication No.72).

KRAMER, H. 1935. Sand mixtures and sand movement in fluvial levels.
Transactions of the American Society of Civil Engineers, 100, 798-838.

KRUMBEIN, W.C. & SLOSS, L.L. 1963. Stratigraphy and sedimentation.
San Francisco: Freeman. 660pp.

LANE, E.W. 1938. Notes on the formation of sand.
Transactions of the American Geophysical Union, 19, 505-508.

MILLER, M.C., McCAVE, I.N. & KOMAR, P.D. 1977. Threshold of sediment motion under unidirectional currents.
Sedimentology, 24, 507-527.

WENTWORTH, C.K. 1922. A scale of grade and class terms for clastic sediments.
Journal of Geology, 30, 377-392.

WILKINSON, R.H. & WAINWRIGHT, B.L.S.A. 1983. A study of proposed sites for wave/current/sediment interaction experiments.
(Private communication).

Instrumentation	Data
Four open toroidal electromagnetic current meter heads (a) 1 at 80cm) (b) 2 at 40cm) (c) 1 at 10cm)	Measurement of orthogonal flow components (a) u',w' (b) u', w', v' (c) u', w'
Compass, pitch and roll sensors	Rig orientation (correction data for orthogonal flow components)
Acoustic backscatter probe	Suspended sediment concentration in various cells above the sea bed
Nunny sediment sampler	Mean suspended sediment concentration during 12 day deployment
Camera and flash	Bedform monitoring
Shrouded current rotor	Mean horizontal current
Current direction sensor	Mean flow direction
Pressure transducer	Tidal fluctuations
Thermistor	Sea temperature

Table 1: STABLE instrumentation, Lundy deployment

Sample	d_{50}	σ_d	SK_d	Ku_d
S_1	2.02	0.140	0.097	0.984
S_2	2.02	0.141	-0.224	1.070
G_1	1.99	0.297	0.397	2.930
G_2	2.15	0.209	-0.093	1.877
G_3	1.92	0.134	-0.319	1.434
G_4	1.96	0.149	-0.155	2.273
BLK	1.97	0.174	0.119	1.615
MEAN VALUE	2.00	0.178	-0.025	1.740

Table 2: Grain size distribution statistics (ø units)

Sample	% carbonates by weight
S_1	10.7
S_2	11.2
G_1	11.9
G_2	11.5
G_3	13.2
G_4	16.1
BLK	12.3
MEAN VALUE	12.4

Table 3: Carbonate component analysis

Bed description	Run	Description of entrainment intensity
FLAT BED	1	Infrequent movement of 'large' (≈700μm) shell fragments as bedload
	2	Sporadic motion of shell fragments and sand grains
	3	Significant particle motion as bedload
	4	All grains in simultaneous motion as a sheet of bedload with the development of bedforms and significant suspension
BED RE-FLATTENED	5	See run 2
	6	Intense bedload transport with most grains entering suspension. Enhanced suspension by vortex shedding from ripple crests.
ASYMMETRICAL RIPPLES	7	Moderate bedload over most of the tipple surfaces with some local shelter
	8	Intense bedload, with some grains entering suspension
	9	Grains entering suspension and intense bedload transport leading to changing ripple geometry
SYMMETRICAL RIPPLES	10	Motion of the first few grains from the ripple crests
	11	Significant entrainment from the ripple crests with intense bedload transport and some suspension

Table 4: Description of sediment dynamics during threshold experiments

Run number	1	2	3	4	5	6	7	8	9	10	11
LDA height above bed (mm)	2	2	2	2	5	5	5	5	5	5	5
ECM height above bed (mm)	50	50	50	50	50	50	60	60	60	60	60
LDA U_{*T}, cms^{-1}	1.28	1.30	1.42	1.68	1.29	1.84	1.28	1.64	1.76	1.16	1.38
Shields criterion, $\Theta_T(x10^{-1})$	4.05	4.18	4.99	6.97	4.11	8.37	4.05	6.65	7.65	3.34	4.70
Grain Reynolds number, Re*	2.46	2.50	2.73	3.23	2.48	3.54	2.46	3.15	3.38	2.23	2.65
ECM U_{50}, cms^{-1}	26.9	28.1	32.0	35.5	28.9	36.7	27.1	37.0	38.7	25.6	29.7
ECM U_{*T}, cms^{-1}	1.24	1.29	1.47	1.63	1.33	--	--	--	--	--	--

Table 5: Sediment threshold values

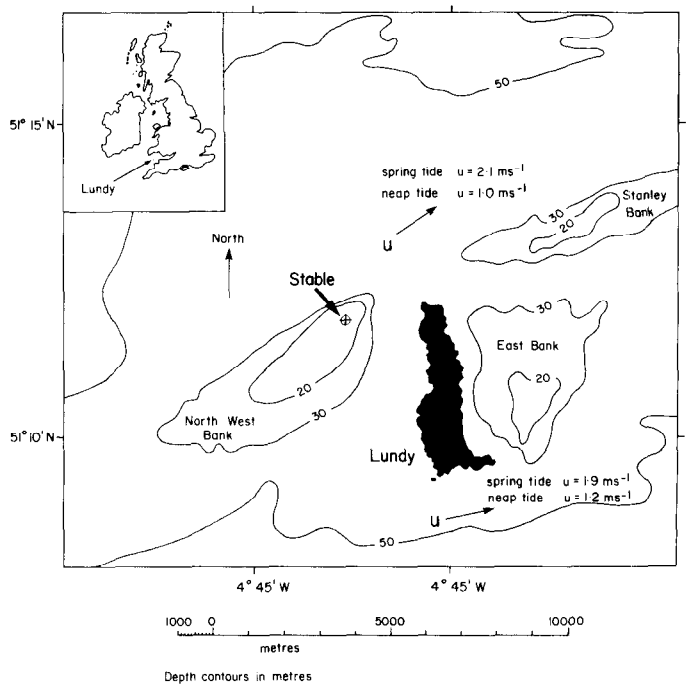

Figure 1. STABLE deployment site, Lundy

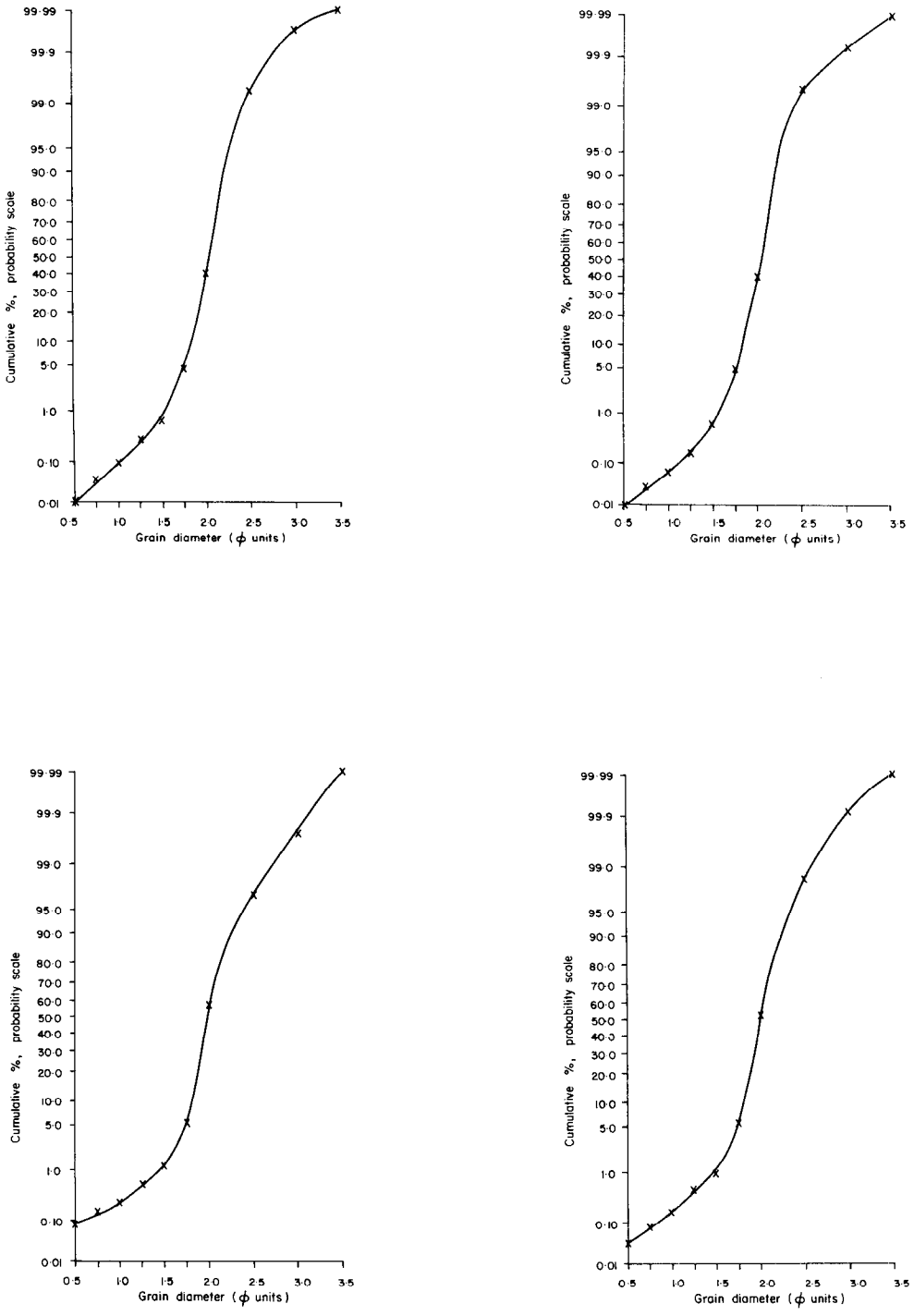

Figure 2. Grain size distribution by dry sieving

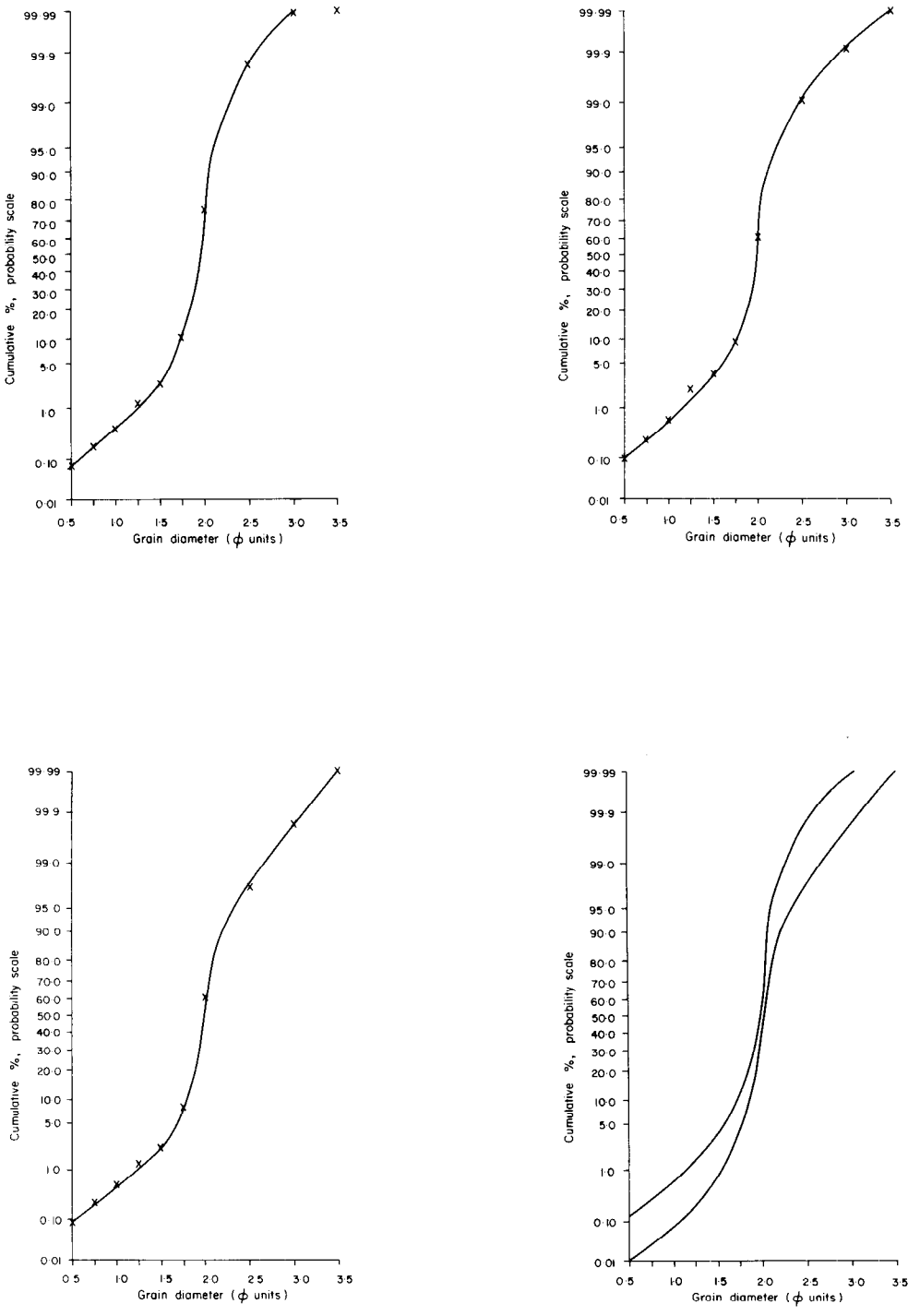

Figure 2 (continued)

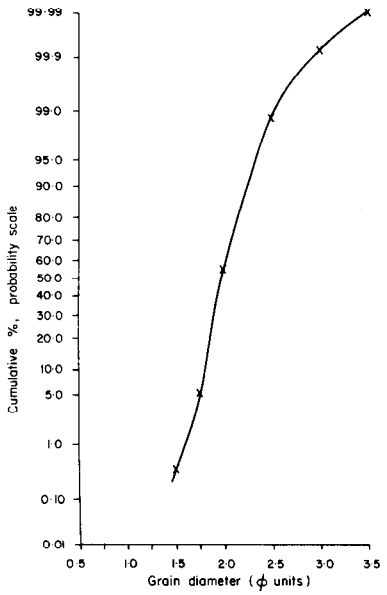

Figure 3. Grain size distribution for carbonate-free sediment

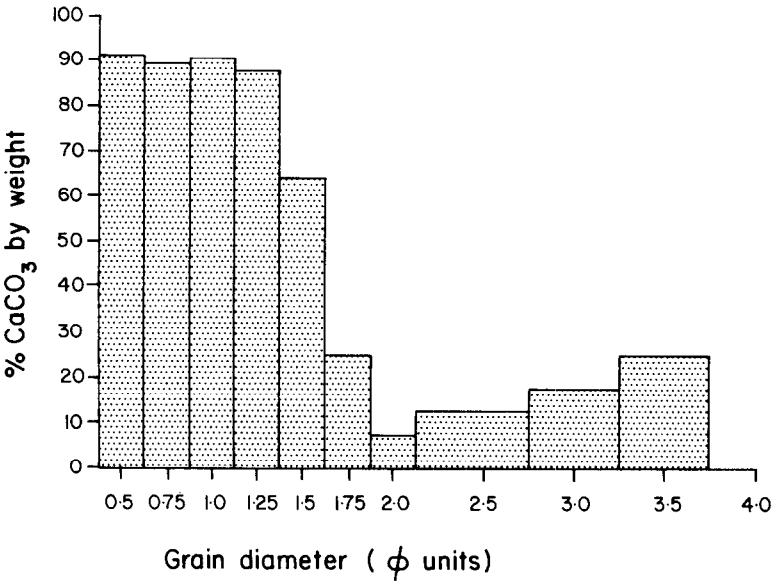

Figure 4. Mean % carbonates in each sieve fraction

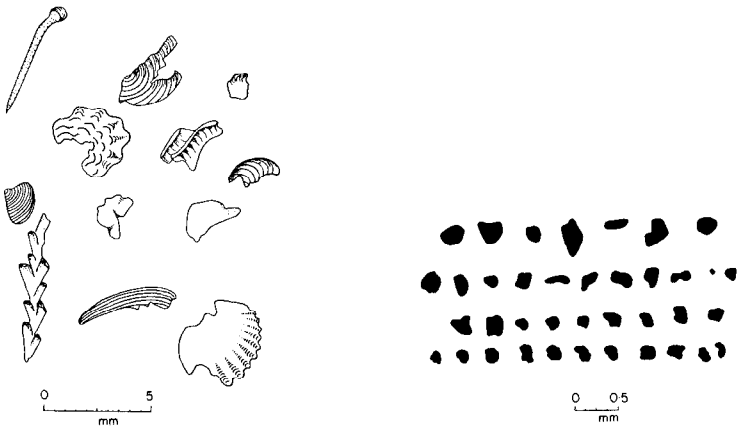

Figure 5. Typical grain shapes: (a) Faunal fragments; and (b) mineral grains

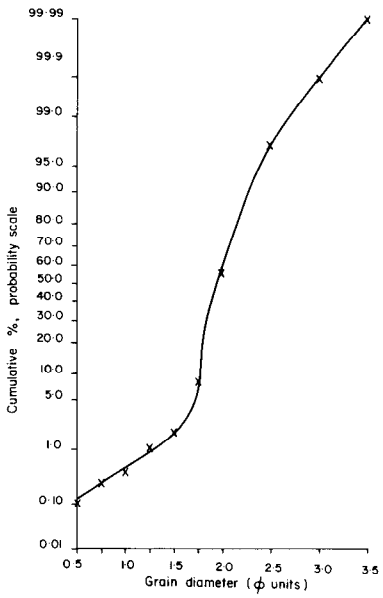

Figure 6. Grain size distribution for suspended sediment

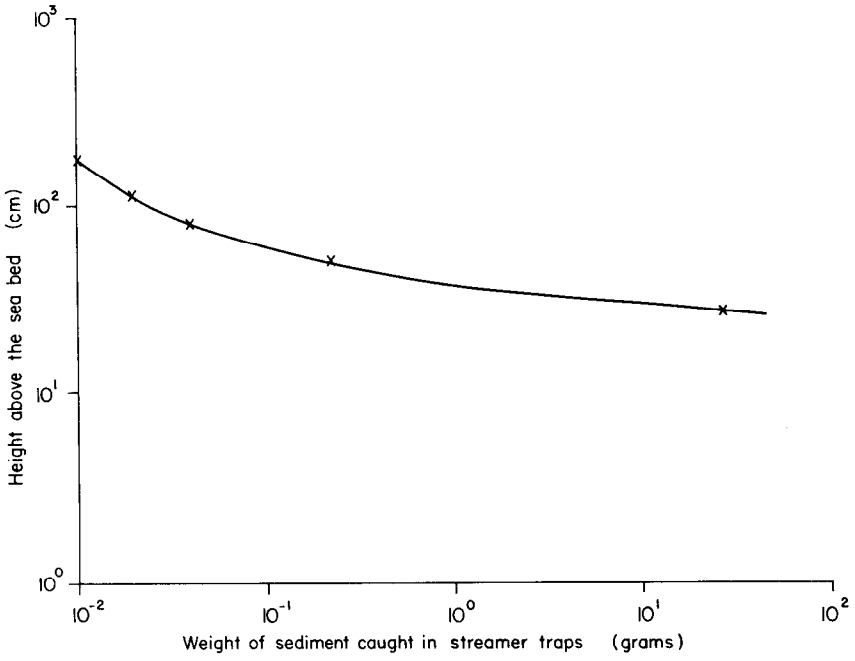

Figure 7. Total suspended sediment profile for $\frac{1}{2}$ hour during maximum ebb tide, 30.09.87

(a) S_1

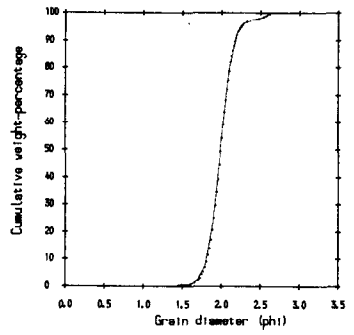

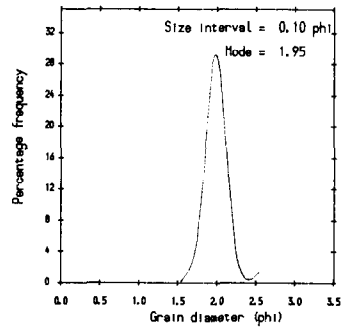

SAMPLE IDENTIFIERS
Date ... 2-11-87
Area ... lundy
Site ...
Sample number s1

(PHI)	MOMENTS	FOLK
Mean	1.974	1.994
Sorting	0.152	0.139
Skewness ...	1.021	0.030
Kurtosis ...	5.040	1.108

VENTWORTH CLASSIFICATION
% gravel 0.0, % sand .. 100.0
% silt .. 0.0, % clay .. 0.0
near-symmetrical,
very well sorted,
medium sand.

(b) S_2

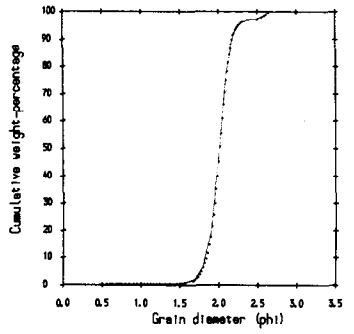

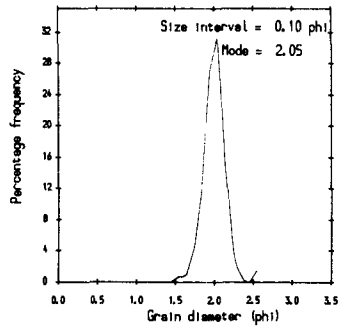

SAMPLE IDENTIFIERS
Date ... 2-11-87
Area ... lundy
Site ...
Sample number s2

(PHI)	MOMENTS	FOLK
Mean	1.975	2.010
Sorting	0.150	0.134
Skewness ...	0.889	-0.016
Kurtosis ...	5.759	1.188

VENTWORTH CLASSIFICATION
% gravel 0.0, % sand .. 100.0
% silt .. 0.0, % clay .. 0.0
near-symmetrical,
very well sorted,
medium sand.

(c) G_1

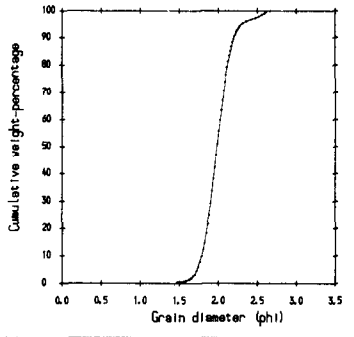

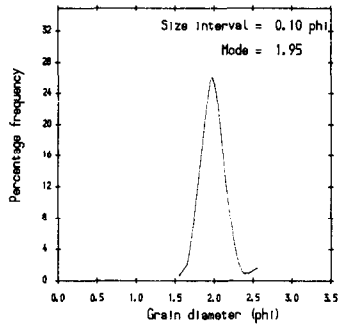

SAMPLE IDENTIFIERS
Date ... 2-11-87
Area ... lundy
Site ...
Sample number g1

(PHI)	MOMENTS	FOLK
Mean	1.966	1.985
Sorting	0.171	0.163
Skewness ...	0.972	0.065
Kurtosis ...	4.419	1.128

VENTWORTH CLASSIFICATION
% gravel 0.0, % sand .. 100.0
% silt .. 0.0, % clay .. 0.0
near-symmetrical,
very well sorted,
medium sand.

Figure 8. Grain size distribution and classification by settling velocity

(d) G_2

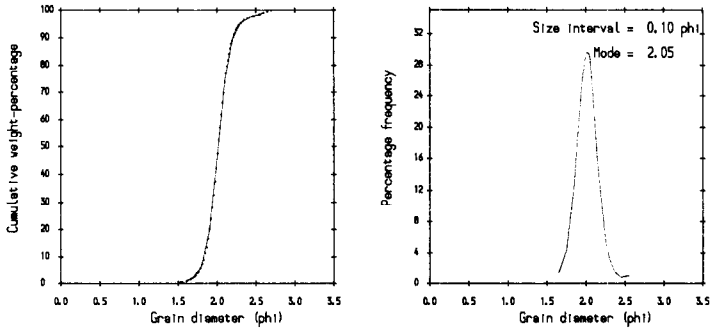

SAMPLE IDENTIFIERS
Date ... 2-11-87
Area ... Lundy
Site ...
Sample number g2

(PHI) MOMENTS		FOLK
Mean	1.983	2.018
Sorting	0.154	0.145
Skewness ...	1.114	0.053
Kurtosis ...	4.459	1.186

WENTWORTH CLASSIFICATION
% gravel 0.0, % sand .. 100.0
% silt .. 0.0, % clay .. 0.0
near-symmetrical,
very well sorted,
medium sand.

(e) G_3

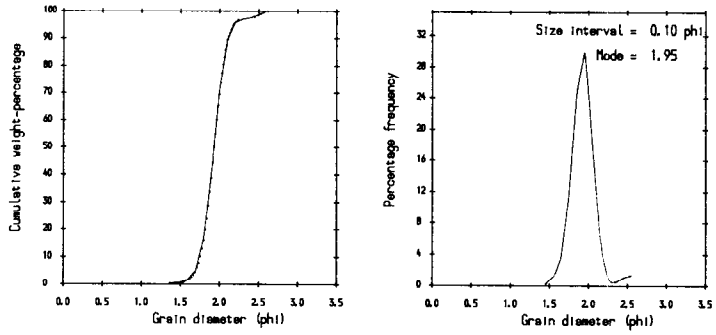

SAMPLE IDENTIFIERS
Date ... 2-11-87
Area ... Lundy
Site ...
Sample number g3

(PHI) MOMENTS		FOLK
Mean	1.927	1.928
Sorting	0.163	0.139
Skewness ...	1.000	0.023
Kurtosis ...	5.792	1.111

WENTWORTH CLASSIFICATION
% gravel 0.0, % sand .. 100.0
% silt .. 0.0, % clay .. 0.0
near-symmetrical,
very well sorted,
medium sand.

(f) G_4

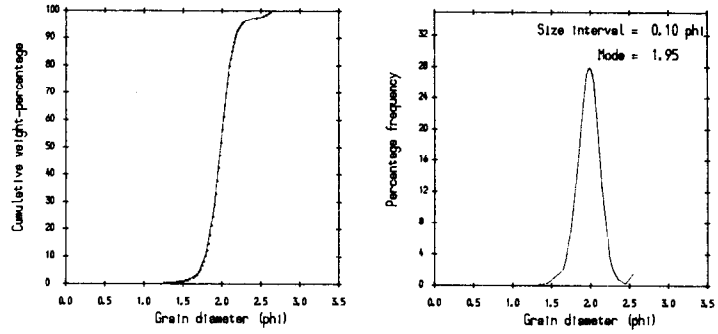

SAMPLE IDENTIFIERS
Date ... 2-11-87
Area ... Lundy
Site ...
Sample number g4

(PHI) MOMENTS		FOLK
Mean	1.955	1.983
Sorting	0.165	0.150
Skewness ...	0.750	-0.009
Kurtosis ...	4.917	1.140

WENTWORTH CLASSIFICATION
% gravel 0.0, % sand .. 100.0
% silt .. 0.0, % clay .. 0.0
near-symmetrical,
very well sorted,
medium sand.

Figure 8 (continued)

(g) BLK

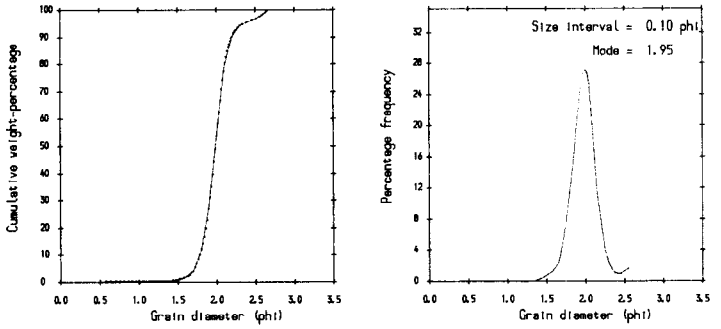

SAMPLE IDENTIFIERS
Date ... 2-11-87
Area ... Lundy
Site ...
Sample number .... b

(PHI) MOMENTS		FOLK
Mean	1.946	1.984
Sorting	0.178	0.169
Skewness ...	0.957	0.040
Kurtosis ...	4.789	1.321

WENTWORTH CLASSIFICATION
% gravel 0.0, % sand .. 100.0
% silt .. 0.0, % clay .. 0.0
near-symmetrical,
very well sorted,
medium sand.

Figure 8 (continued)

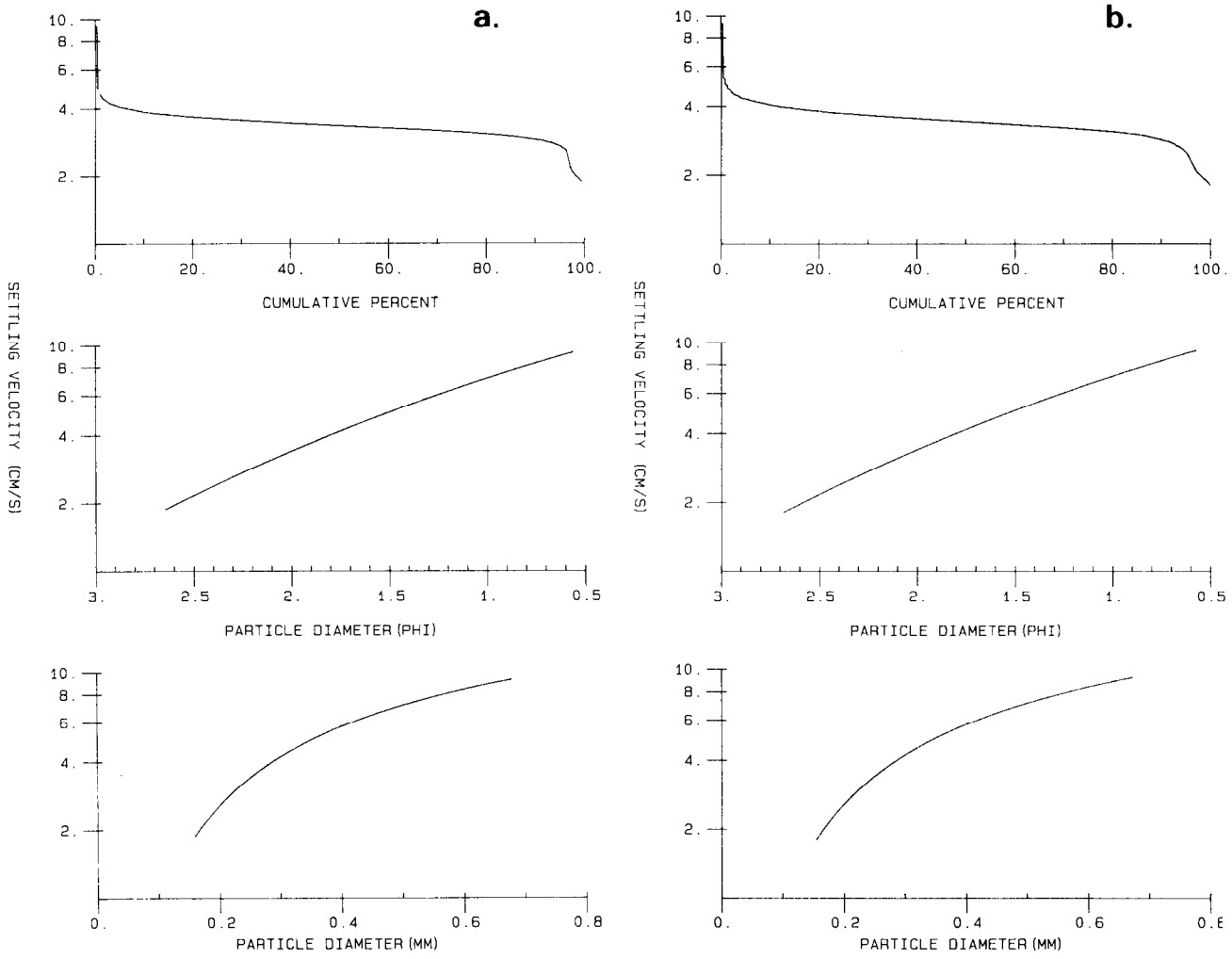

Figure 9. Mean grain size and settling velocity distributions: (a) Surface samples; and (b) Grab samples

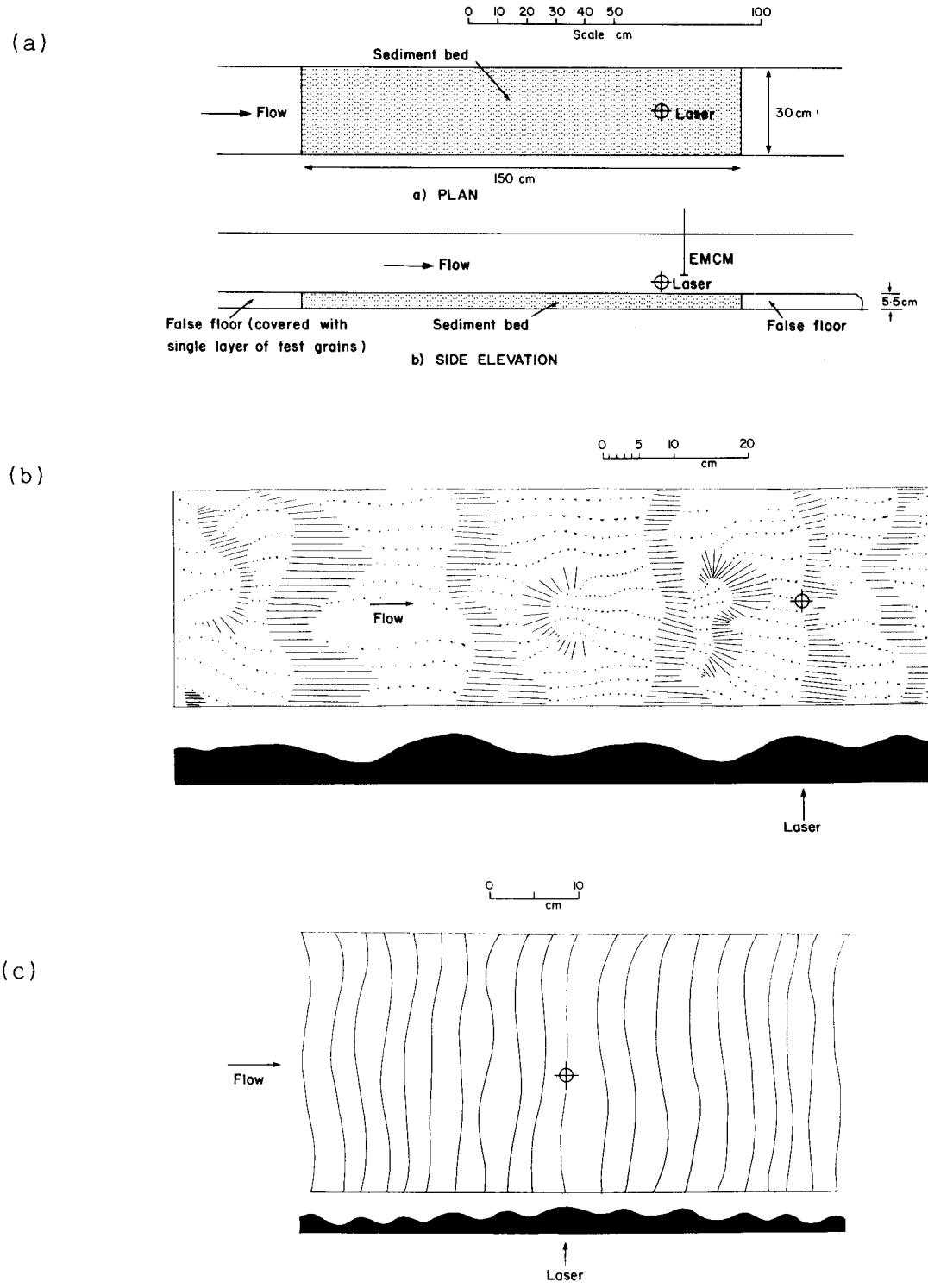

Figure 10. Bed configuration for threshold experiments: (a) Flat bed; (b) Asymmetrical ripples; and (c) Symmetrical ripples

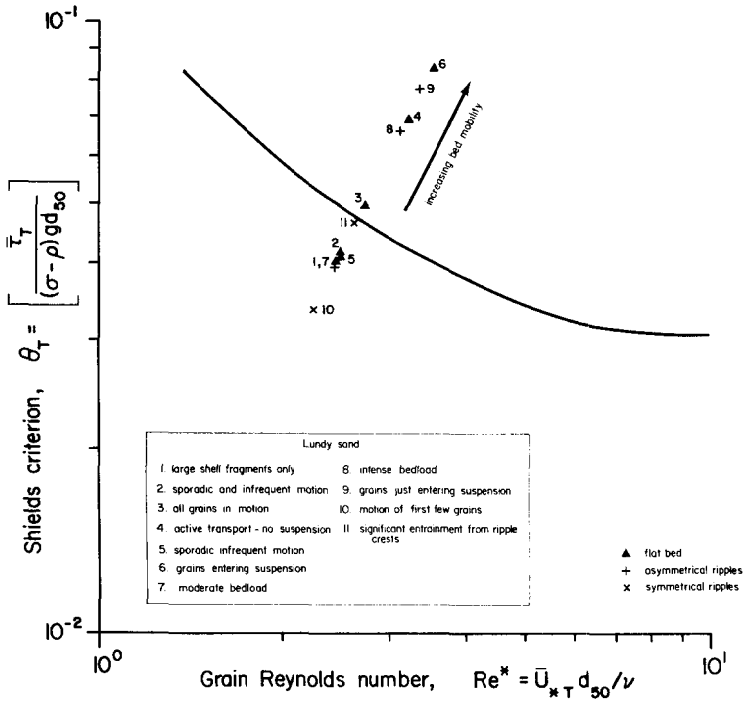

Figure 11. Shields curve showing threshold data for Lundy sand